Detection and Analysis of Microfronts and Associated Coherent Events Using Localized Transforms

NIMAL GAMAGE*

Department of Atmospheric Sciences, Oregon State University, Corvallis, Oregon

CARL HAGELBERG**

Department of Mathematics, Oregon State University, Corvallis, Oregon

(Manuscript received 20 June 1991, in final form 4 May 1992)

ABSTRACT

A general localized transform is used to study the characteristics of conditional sampling techniques. A covariance transform is defined that measures the covariance between the signal and a dilated and translated generating function which has compact support. It is shown to be superior as a method of detecting events containing sharp edges such as fronts or microfronts when compared with energy-preserving transforms such as the Fourier and wavelet transform. A method of finding the most coherent scale with respect to dilation of the generating function is presented. A sample analysis using sonic data measured in shear driven boundary-layer atmospheric turbulence is presented.

1. Introduction

Sharp transitions in temperature, moisture, and velocity fields, with respect to space or time, are important features of geophysical turbulence. It is therefore desirable to identify and characterize zones in sampled signals where these microfront transitions occur. For example, Antonia and Atkinson (1976), Antonia and Van Atta (1978), and Schols (1984) report on analysis of such microfront-related coherent structures. The Introduction in Mahrt (1991) gives an overview of the current literature regarding the interest and observations of sharp transitions in atmospheric turbulence.

Various methods for the identification of microfronts in data have been proposed (Mahrt 1991; Schols 1984; Bergström and Högström 1989; Taubenheim 1989). Each method relies on some type of localized transform as part of the event-finding process. Mahrt (1991) gives a method based on a variant of the wavelet transform developed in Daubechies (1988). Other widely used methods for identifying sharp transitions are the VITA method (Schols 1984; Bergström and Högström 1989) and a method based on localized variance (Taubenheim 1989). In this paper, we show that the localized transform as defined by Arneodo et al. (1989) is the most general type of transform and that each of the other transforms may be derived by a particular choice of transform parameters. We show that in the detection and analysis of microfront-related coherent events there is an ideal choice of scaling and basis set that can be interpreted in terms of the covariance and correlation. We define this as the *covariance transform.*

In Fourier analysis the signal is decomposed into components of a basis set. Each element of the basis is nonzero on the entire domain except at distinct zero crossings. The transform coefficients are influenced by the entire signal and therefore do not have a direct relationship to localized events in the signal. Hence, the Fourier transform is a "global" transform. To obtain a localized relationship, a decomposition into a localized basis, which is parametrized by scale and position, is needed. The wavelet transform (Meyer 1989; Grossmann et al. 1989; Daubechies 1988) and transforms closely related to it (Arneodo et al. 1989) have the desired properties.

The wavelet transform and its variants are characterized as "local" transforms because the basis elements that define the transform coefficients have compact (i.e., closed and bounded) support. The support of a function is the set on which the function is not zero. This localization, in space or time, means that the transform is only influenced by a portion of the signal localized around the point defined by the translation parameter. Hence, the transform coefficients will have a direct relation to the local behavior of the signal (Meyer 1989).

Parseval's theorem in the theory of Fourier transforms is the statement that the variance in the signal

* *Current affiliation:* Department of Astrophysical, Planetary, and Atmospheric Sciences, University of Colorado, Boulder, CO.

** *Current affiliation:* National Center for Atmospheric Research.

Corresponding author address: Dr. Nimal Gamage, Department of Astrophysical, Planetary, and Atmospheric Sciences, University of Colorado, Campus Box 391, Boulder, CO 80309.

can be obtained as a sum of the squared transform coefficients. The magnitude of a given Fourier coefficient is a direct indication of the amount of variance of the record explained by that mode. In general, a transform is an *isometry* if it preserves the L^2 norm (in velocity records this would be the energy). Parseval's theorem holds because the Fourier transform is an isometry. The wavelet transform given by Daubechies (1988) is also an isometry. We show that the choice of scaling used in Mahrt (1991) is not an isometry. This means that the transform used in Mahrt (1991) is not a decomposition of the signal variance. We show, however, that such a transform is optimal when trying to identify structures associated with sharp transitions. The effect of scaling on the local transform was alluded to in Arneodo et al. (1989), and this effect is clarified for this application.

In section 2, we develop the terminology and theoretical relationships among the transforms of interest. Section 3 compares microfront detection methods using idealized artificial data. Section 4 makes a comparison of the techniques from sections 2 and 3.

2. Theoretical considerations

A basis can be constructed by specifying a *generating function,* $h(x)$, where x denotes space or time and could be multidimensional. For the following development, we will assume x to be a one-dimensional variable. The function $h(x)$ is chosen to meet certain *admissibility criteria* (Meyer 1989; Grossmann et al. 1989) given by

(i) zero mean: $\int h(x)dx = 0$, and
(ii) adequate decay in frequency space:

$$\int |\omega|^{-1}|\hat{h}(\omega)|^2 d\omega < \infty,$$

where $\hat{h}(\omega)$ is the Fourier transform of $h(x)$.

In addition to the admissibility criteria,

$$\frac{1}{l}\int h(x)h(x)dx = 1, \qquad (1)$$

where l is the support of $h(x)$.

The basis set used for the transformation is generated by translations, $h(x) \mapsto h(x - b)$, and dilations, $h(x) \mapsto h(x/a)$ of the generating function. In this development we restrict our attention to a particular admissible h, represented by a Haar function. An arbitrary element of the Haar basis $h_{a,b}(x)$ is given by

$$h\left(\frac{x-b}{a}\right) = \begin{cases} -1, & b - \frac{a}{2} \leq x \leq b \\ 1, & b \leq x \leq b + \frac{a}{2} \\ 0, & \text{elsewhere.} \end{cases} \qquad (2)$$

This is a step centered at b spanning a length of a.

The *localized transform* $W_f(a, b)$ of a function $f(x) \in L^2(\mathbb{R})$, using the basis defined in Eq. (1), is defined as

$$W_f(a, b)|_p = a^{-p}\int_{-\infty}^{\infty} f(x)h\left(\frac{x-b}{a}\right)dx, \qquad (3)$$

where the parameter p will be referred to as the normalizing factor.

The two cases $p = 1/2$ and $p = 1$ are considered since they can be used to generate the transforms used in many conditional sampling schemes. When $p = 1/2$, Eqs. (2) and (3) define the *wavelet transform* (Meyer 1989; Grossman et al. 1989; Daubechies 1988). The wavelet transform is an isometric, unitary mapping from $L^2(\mathbb{R}) \mapsto L^2(\mathbb{R}\backslash 0 \times \mathbb{R})$, where L^2 denotes the space of functions that are square integrable over the domain consisting of the reals, $\mathbb{R}$, or the x, y plane excluding $y = 0$. The range of this map is defined as the *wavelet phase plane.* A point on the wavelet phase plane represents the value of the transform at a given translation, b, and dilation, a. Equation (3) defines a norm-preserving mapping (Grossmann and Morlet 1987), that is,

$$\|f\|_{L^2} = \|W_f(a, b)|_{1/2}\|_{L^2} = \int_0^{\infty}\int_{-\infty}^{\infty} [W_f(a, b)|_{1/2}]^2 db\, da. \qquad (4)$$

Parseval's theorem implies that the variance of f can be expressed as a function of dilation by integrating (4) over b (Gamage 1990b). This decomposition is defined as the *wavelet variance* at dilation a, given by

$$D^2(a)|_{1/2} = \int_{-\infty}^{\infty} [W_f(a, b)|_{1/2}]^2 db. \qquad (5)$$

Equation (5) gives the variance of $W_f(a, b)$ in the phase plane for a fixed a. The wavelet variance can be compared to a Fourier decomposition, where the variance of the signal is decomposed into a function of wavelength. The main difference between the wavelet and the Fourier decompositions is in the support of the respective basis functions. The wavelet transform coefficients are influenced by the local events, while the Fourier coefficients are influenced by the signal on its entire domain. This makes the wavelet variance a better measure of variance attributed to localized events.

When $p = 1$, Eqs. (2) and (3) define a transform that will be called the *covariance transform.* The covariance transform is an injective (one-to-one) mapping from $L^2(\mathbb{R}) \mapsto L^2(\mathbb{R}\backslash 0 \times \mathbb{R})$. The range of the map, in this case, is defined as the *covariance phase plane.* The covariance transform is not norm-preserving (i.e., not isometric) since the L^2-norm in the covariance phase plane of $W_f(a, b)|_1$ is not equal to the L^2-norm of the signal. That is,

$$\|W_f(a,b)|_1\|_{L^2} = \int_0^\infty \int_{-\infty}^\infty [W_f(a,b)|_1]^2 db da$$

$$= \int_0^\infty \frac{1}{a}\left[\int_{-\infty}^\infty [W_f(a,b)|_{1/2}]^2 db\right] da$$

$$= \int_0^\infty \frac{1}{a}[D^2(a)|_{1/2}] da \quad (6)$$

$$\neq \|f\|_{L^2}. \quad (7)$$

The inequality in Eq. (7) follows from (4) and (5). The covariance between an arbitrary function f and the function h [Eq. (2)] can be defined as

$$\mathrm{cov}_{f,h}(a,b) = \frac{1}{a}\int_{b-a/2}^{b+a/2} f(x)h\left(\frac{x-b}{a}\right)dx. \quad (8)$$

The correlation between the two functions, f and h, is then given by

$$r_{f,h}(a,b) = \frac{\mathrm{cov}_{f,h}(a,b)}{[\mathrm{cov}_{f,f}(a,b)\,\mathrm{cov}_{h,h}(a,b)]^{1/2}}. \quad (9)$$

Using Eqs. (8) and (9), Eq. (3) with $p = 1$ can be written as

$$W_f(a,b)|_1 = \mathrm{cov}_{f,h}(a,b) \quad (10)$$

$$= r_{f,h}(a,b)[\mathrm{cov}_{f,f}(a,b)\,\mathrm{cov}_{h,h}(a,b)]^{1/2}. \quad (11)$$

Note that for the Haar function [Eq. (2)] considered here, $\mathrm{cov}_{h,h}(a,b) = 1$. Hence, (11) becomes

$$W_f(a,b)|_1 = r_{f,h}(a,b)[\mathrm{cov}_{f,f}(a,b)]^{1/2}. \quad (12)$$

In Eq. (12), $r_{f,h}$ is a measure of the similarity in shape between f and h in the neighborhood of b. Positive values of $r_{f,h}$ indicate an in-phase similarity and negative values an out-of-phase similarity. However, $r_{f,h}$ will equally weight signals of arbitrary amplitude but of similar shape. This means that it cannot distinguish "noise level" signals from "events." Here $\mathrm{cov}_{f,f}(a,b)$ is a measure of the variance of the signal in the neighborhood of b, and provides a means of *distinguishing* between "noise level" signals and "events." Hence, $W_f(a,b)|_1$ is a measure of both the similarity between the basis function h and the signal f and the variance of f in the neighborhood of b. Our choice of h as a Haar function is motivated by an effort to locate "events" in the signal that are characterized by sharp transitions in conjunction with large variance, such as microfronts. Constructing a measure similar to (5) for the case $p = 1$ gives

$$D^2(a)|_1 = \int_0^\infty [W_f(a,b)|_1]^2 db$$

$$= \int_0^\infty [r_{f,h}]^2[\mathrm{cov}_{f,f}] db. \quad (13)$$

Since (3) with $p = 1$ does not define a norm-preserving map, (13) is not a variance decomposition. It is, however, a representation of the distribution of $W_f(a,b)|_1$ with dilation a. Since $W_f(a,b)|_1$ is a measure of the similarity of f and h, (13) provides an indication of the scale of the most coherent events that have the characteristics of h.

3. Microfront detection

Localized transform methods have been used as an event-finding mechanism in several studies (Bergström and Högström 1989; Schols 1984; Mahrt 1991). Equation (12) defines a general localized transform that can now be used to study the characteristics of different conditional sampling techniques. In an event-finding mechanism, the transformed variable is compared to a transform of a known signal or to a threshold value.

The transform used in the VITA method can be obtained from (12) if

$$h\left(\frac{a-b}{a}\right) = f'(x) \quad \text{for} \quad b - \frac{a}{2} \leq x \leq b + \frac{a}{2},$$

where

$$f'(x) = f(x) - \frac{1}{a}\int_{b-a/2}^{b+a/2} f(x)dx.$$

For this case, $r_{f,h}$ is unity and (12) is a measure of the local variance. Thus, in the VITA method, an elevated localized region of variance is used as the conditional sampling mechanism. Since the VITA method is not a projection onto a fixed basis, it is not a decomposition of the original signal. This implies that the VITA method cannot be used as a filtering mechanism, where a partial reconstruction of the signal is achieved through the inverse transform of a few modes. Furthermore, since it has no built-in knowledge of a microfront event, it is unable to differentiate microfront events from other high-variance events.

If $p = 1$ and h is defined by (2), the covariance transform [Eq. (3)] can be used as an event finding mechanism. Consider the idealized artificial signal, located at $x = 0$, shown in Fig. 1. The *sharpness scale* of the microfront is labeled as σ and the width of the microfront related coherent event is τ. The covariance transform for this signal at $b = 0$ is

$$W_f(a,0)|_1 = \begin{cases} \dfrac{a}{2\sigma}, & a \leq \sigma \\ \dfrac{\sigma}{2a} + \dfrac{a-\sigma}{a}, & \sigma \leq a \leq \tau \\ \dfrac{1}{a}\left(\tau - \dfrac{\sigma}{2}\right), & \tau \leq a. \end{cases} \quad (14)$$

The maximum value of the transform is at $a = \tau$. When $\sigma = 0$, the microfront is a step signal and the transform

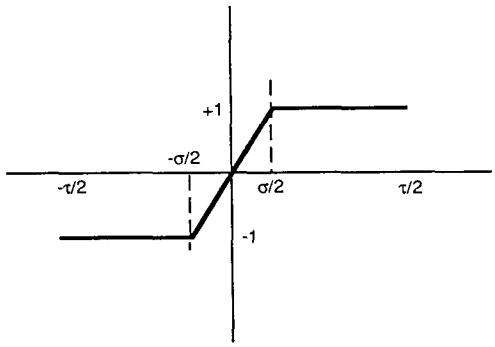

FIG. 1. Idealized microfront test signal located at $b = 0$. Sharpness scale of the microfront is defined as σ; coherent event width is τ.

remains constant $[W_f(a, 0)|_1 = 1]$ for all dilations less than τ. When $\sigma > 0$, that is, the signal has a finite width microfront, the transform becomes smaller than the value at $a = \tau$ for dilations smaller than τ. At dilation $a = \sigma$, the transform $W_f(\sigma, 0)|_1 = 0.5$ for all $\sigma \geq 0$.

The above analysis can be extended to $W_f(a, 0)|_p$ for any $p > 0$. The decay of the transform, $W_f(a, 0)|_p$, for dilations a less than τ is a measure of the sharpness of the microfront. Figure 2 shows plots of the transform with (a) $p = 1/2$, (b) $p = 1$, and (c) $p = 2$. The slope of a given segment is the rate of change of the log of the transform of a particular shape with respect to the log of the scale. For $p = 1$, this can be interpreted as the rate of change of covariance with respect to dilation. In each case (Figs. 2a–c), a change in slope indicates that the transform has reached the scale of a different structure in the signal. For example, in Fig. 2b, the slope is approximately 1.5 where the scale of the transform is only large enough to be affected by the transition zone of the microfront. There is then a relatively short transition to a segment with nearly zero slope where the scale has now become large enough to register the entire Haar function event, including the microfront. The beginning of the transition from slope 1.5 towards slope zero corresponds to the sharpness scale $a = 1/2$. Finally, there is a sharp transition to a segment with a slope of approximately -0.5, where the scale has become larger than the total coherent event.

Comparison of the three transforms, $p = 0.5$, $p = 1$, and $p = 2$ shows that the best scale isolation of the microfront and the coherent event is provided by $p = 1$. The nearly constant value of the transform between the sharpness scale and the coherent-event scale also allows for a threshold value–based detector. Since $W_f(a, b)|_1$, with h defined in Eq. (2), is a measure of the similarity of the signal to a Haar function at a given translation, and a measure of the sharpness (Eq. 14) and scale of the coherent event associated with the microfront, it provides a microfront event-finding mechanism.

In conditional sampling methods the first task is to find the length scale of the coherent events at which to compute the transform. In the case of atmospheric turbulence these coherent events may be spaced nonperiodically. The Fourier spectrum is unable to detect the scales of this type of event accurately since it decomposes the signal into a globally defined basis. Thus, the choice of the averaging length scale, if based on spectral peaks, is not at the scale of maximum variance of the coherent structures (Gamage 1990a). In the covariance transform method the global statistic constructed in Eq. (13) provides the scale of maximum covariance of the coherent structures (Gamage 1990a,b). This measure is superior to the wavelet variance (3) in the detection of the scale of the coherent structures, even though the wavelet variance is also a localized transform. The normalizing factor p in Eq. (3) affects the scale-discrimination properties of the transform plane [a detailed analysis of this is given in Arneodo et al. (1989)]. Figure 3 shows the wavelet variance [$p = 1/2$, Eq. (5)] and the covariance decomposition [$p = 1$, Eq. (13)] for two artificial signals of randomly spaced events as a function of dilation. The

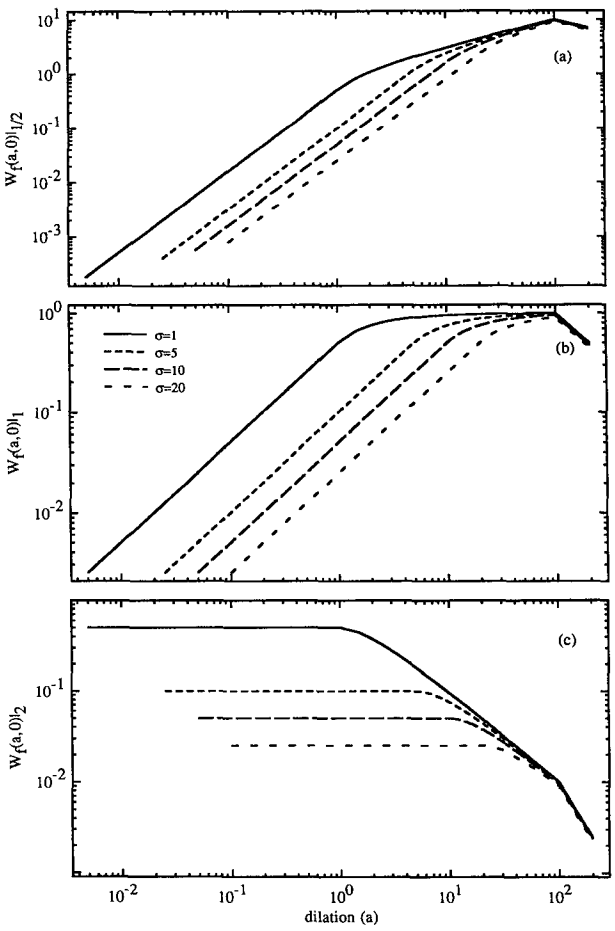

FIG. 2. Transform, $W_f(a, b)|_p$, at $b = 0$ of the idealized microfront event (Fig. 1) for sharpness scale $\sigma = 1, 5, 10, 20$ and event width $\tau = 100$: (a) $p = 1/2$, (b) $p = 1$, (c) $p = 2$.

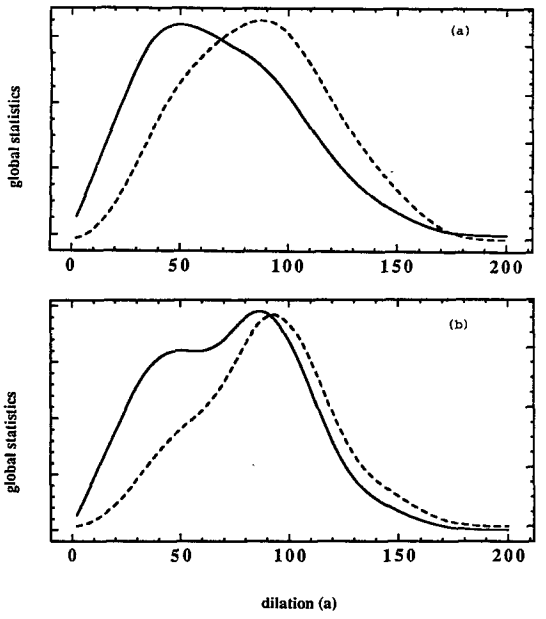

FIG. 3. (a) Wavelet variance $D^2(a)|_{1/2}$ (solid line) and global statistics of the covariance transform $D^2(a)|_1$ (broken line) for a test signal consisting of top-hat events each 50 points wide randomly distributed with a mean spacing of 200 points. The top-hats are of amplitude unity. (b) Same as (a) but with top hats replaced by sine pulses on $[0, \pi]$ as the events.

peak in the covariance decomposition is at the scale of the coherent events (the width of the events). The wavelet variance peak is at an unrelated scale. This difference in location of the peaks occurs as a result of 1) the wavelet variance being a decomposition of the variance and not of the covariance with the basis set and 2) larger values of p providing better-scale separation in the transform phase plane. Thus, the covariance decomposition provides a method of determining the length scale of the coherent events to be used in conditional sampling schemes.

4. Example analysis using observed data

As an example, we analyze a portion of the atmospheric time series data gathered during the Lam mefjord experiment conducted in Denmark in 1987–88 (Courtney 1987). A 50-hour segment of u (in the direction of the mean wind), v and w wind velocity time series collected during a period of strong uniform winds in June 1987, is analyzed. The data was sampled at 16 Hz using a sonic anemometer mounted on top of a 45-m tower. Detailed description of the site is given in Courtney (1987) and of the instrumentation in Courtney (1987) and Mortensen et al. (1987). During the 50-hour period the mean wind was 12 m s^{-1} and of uniform direction.

The global statistics of the covariance transform (Eq. 13) computed for the three velocity components are shown in Fig. 4. The dilation of peak covariance in the

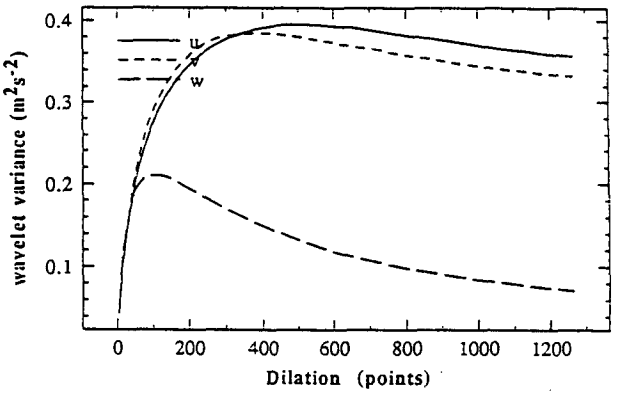

FIG. 4. $D^2(a)|_1$ computed for the three velocity components in the LAMEX 50-hour data.

u component at 500 points is chosen as the length scale for conditional sampling. Although the peak in w is better defined than that of u, the u time series is chosen for the conditional sampling since the turbulence is driven by the horizontal shear. Samples are collected by applying a threshold value of zero to the covariance transform computed at $a = 500$, $W_f(500, b)|_1$. The samples have no overlap with one another. Three independent sets of samples are selected using the covariance transform computed with the Haar generating function, the single sine pulse on $[-\pi, \pi]$ as the generating function, and the single sine pulse on $[-\pi/2, \pi/2]$ as the generating function. A fourth sample using the VITA method applied at a 500-point length scale is also collected. For each case approximately 2200 nonoverlapping sample locations were selected.

Figure 5 shows a plot of the composite event of the samples. The samples are individually demeaned prior to averaging. The samples are centered at the microfront and extend 354 points in each direction. The width of the coherent event as given by the peak in the global statistics computed by Eq. (13) (Fig. 4) agrees with the width of the composite in u. As seen in the composite of w, the microfront in u is associated with

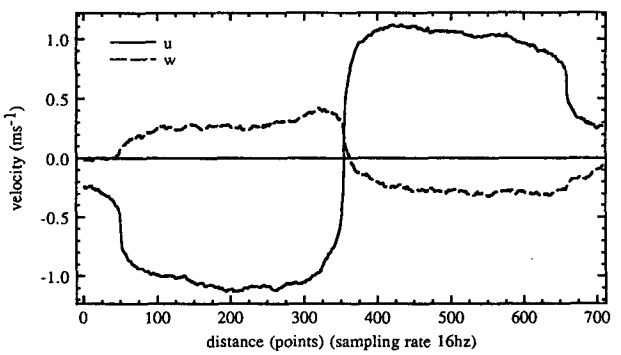

FIG. 5. Plot of composite of microfront events sampled from LAMEX using the covariance transform at 608-point dilation. The sampling is based on the u velocity.

a weaker microfront in w. The w samples composited here, however, are not the ones corresponding to the peak in the global statistics in w but the samples corresponding to the peak in u. Hence the w composite corresponds to a weak "nonevent." An attempt to discover the sharpness scale of the composite using different values of p shows that $p = 1$ differentiates the sharpness scale from the event scale most clearly, Fig. 6. The beginning of the zero-slope portion of Fig. 6b at approximately 200 points corresponds to the sharpness scale (σ) of the microfront, while the end of the zero-slope portion at 600 points corresponds to the coherent-event scale.

Since the eigenvectors of the lagged covariance matrix computed from the samples form a covariance maximizing basis (in L^2) for the samples (Petersen 1976; Panofsky and Dutton 1984; Mahrt and Frank 1988), we compute them as a means of evaluating the conditional sampling methods. The successive eigen-

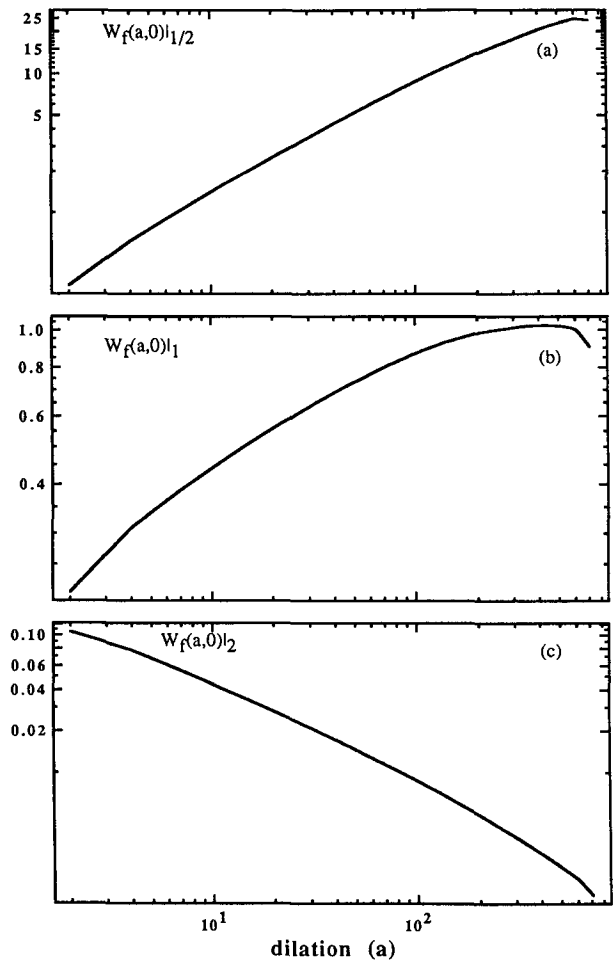

FIG. 6. (a) $W_f(a, 0)|_{1/2}$, (b) $W_f(a, 0)|_1$, and (c) $W_f(a, 0)|_2$ of the u velocity of composite event versus dilation. The coherent event scale is most easily seen in (a) and (b), while sharpness scale is only evident in (b).

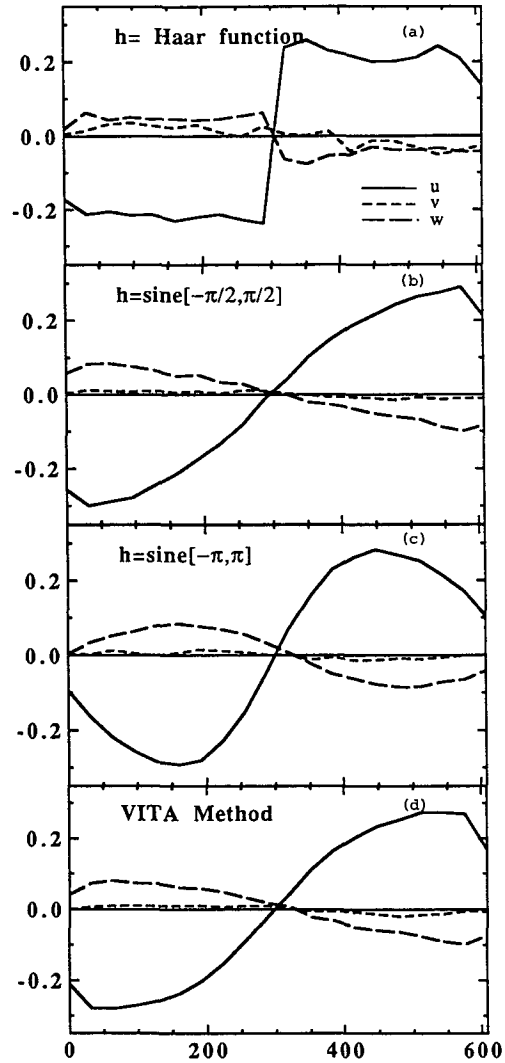

FIG. 7. The first eigenvector of the samples for the u, v, and w velocity components. (a) Samples selected using the Haar generating function and the covariance transform. (b) Samples selected using the $\sin[-\pi/2, \pi/2]$ generating function and the covariance transform. (c) Samples selected using the $\sin[-\pi, \pi]$ generating function and the covariance transform. (d) Samples selected using the VITA method.

vectors maximize the residual covariance. The first eigenvector of the three velocity components for each of the sampling methods is shown in Fig. 7. The first eigenvector explains 23%–28% of the variance in the samples selected. In each case, the sampling is based on the u component only. Thus, the v and w components do not reflect the characteristics of the sampling technique. A detailed description of the method of computing these eigenvectors is given in Mahrt (1991). Figures 7a,b,c show that the first eigenvector of the sampled variable mimics the generating function used in the covariance transform. The first eigenvectors describe the characteristics of the sampled events in terms

of the velocity components. Figure 7a suggests that microfront events in u are associated with weak microfronts in w. This confirms the effectiveness of the sampling method, which is expected due to the covariance maximizing characteristic of the covariance transform sampling method.

In the VITA method of sample selection (Fig. 7d), the first eigenvector of the sampled variable indicates a smooth event similar to a sine pulse (Fig. 7b). The variance maximizing nature of the VITA method is unable to detect the microfront events in the record. Instead, the sampling finds the characteristics of the most energetic events in terms of variance regardless of coherence.

5. Conclusions

The definition of the covariance transform given provides a natural link between several conditional sampling techniques. This provides insight into the characteristics of these sampling techniques and a means for selecting the technique for a specific application. The analysis presented here suggests that the detection of the scales associated with nonperiodically spaced coherent structures is best accomplished by the use of the global statistics of the covariance transform. When the coherent events can be described by some characteristic physics, such as being associated with a microfront, the covariance transform provides a preferred method for the detection of such events. The wavelet transform and the VITA method do not provide a method of discriminating between sharp transitions and other energetic events and cannot be used for the detection of sudden transitions or their associated scales.

Acknowledgments. The numerous discussions and helpful comments of Larry Mahrt and computational assistance of Wayne Gibson is greatly appreciated. Nimal Gamage's work was supported by the United States Army Research Office under Contract DAA-03089-k-0113.

REFERENCES

Antonia, R. A., and J. D. Atkinson, 1976: A ramp model for turbulent temperature fluctuations. *Phys. Fluids,* **19,** 1273–1278.

——, and C. W. Van Atta, 1978: A ramp model for turbulent temperature fluctuations. *J. Fluid Mech.,* **84,** 561–580.

Arneodo, A., G. Grasseau, and M. Holschneider, 1989: Wavelet analysis of invariant measures of some dynamical systems. *Wavelets,* Springer-Verlag, 315 pp.

Bergsrtöm, H., and U. Högström, 1989: Turbulent exchange above a pine forest, Part II. Organized structures. *Bound.-Layer Meteor.,* **42,** 941–949.

Courtney, M. S., 1987: The Lammefjord experiment. *Proc. 1987 American Wind Energy Association Annual Conf.,* San Francisco, Amer. Wind Energy Assoc., 23–37.

Daubechies, I., 1988: Orthonormal basis of compactly supported wavelets. *Commun. Pure Appl. Math.,* **41,** 909–996.

Gamage, N., 1990a: Modelling and analysis of geophysical turbulence: Use of optimal transforms and basis sets. Ph.D. thesis. Oregon State University, 135 pp. [Available from University Microfilm, 305 N. Zeeb Rd., Ann Arbor, MI 48106.]

——, 1990b: Detection of coherent structures in shear induced turbulence using wavelet transform methods. Preprints, *Ninth Symp. on Turbulence and Diffusion,* Roskilde, Amer. Meteor. Soc., 453–454.

Grossmann, A., and J. Morlet, 1987: Decomposition of functions into wavelets of constant shape and related transforms. *Lectures on Recent Results on Mathematics and Physics.* World Scientific, 165 pp.

——, R. Kroland-Martinet, and J. Morlet, 1989: Reading and understanding continuous wavelet transforms. *Wavelets,* Springer-Verlag, 315 pp.

Mahrt, L., 1991: Eddy asymmetry in the sheared heated boundary layer. *J. Atmos. Sci.,* **48,** 472–492.

——, and H. Frank, 1988: Eigenstructure of eddy microfronts. *Tellus,* **48A,** 107–119.

Meyer, Y., 1989: Orthonormal wavelets. *Wavelets,* Springer-Verlag, 315 pp.

Motensen, N. G., S. E. Larson, I. Toren, and T. Mikkelsen, 1987: Two years worth of turbulence data recorded by sonic anemometer based data acquisition system. *Proc. Sixth Symp. Meteor. Observations and Instrumentation,* New Orleans, Amer. Meteor. Soc., 201–202.

Panofsky, H. A., and J. A. Dutton, 1984: *Atmospheric Turbulence.* Wiley and Sons, 397 pp.

Petersen, E. L., 1976: A model for the simulation of atmospheric turbulence. *J. Appl. Meteor.,* **15,** 571–578.

Schols, J. L. J., 1984: The detection and measurement of turbulent structures in the atmospheric surface layer. *Bound.-Layer Meteor.,* **29,** 39–58.

Taubenhiem, J., 1989: An easy procedure for detecting a discontinuity in a digital time series. *Z. Meteorol.,* **39,** 344–347.